Supplementary data

List of Ev-AIFib sites

Hôpital Saint-Joseph, Marseille, France
Centre Cardiologique du Nord, Saint-Denis, France
Centre Hospitalier Universitaire de Nice, Nice, France
Clinique Ambroise Paré, Neuilly-sur-Seine, France
Clinique Pasteur, Toulouse, France
Hôpital Privé Jacques Cartier, Massy, France
Hôpital Saint-Philibert, Lomme, France
Infirmerie Protestante, Caluire-et-Cuire, France

Methods

More details on VX1

VX1 relies on the off-line pre-training of multiparametric deep and machine learning algorithms on a database of annotated AF intra-cardiac electrograms. This training database of >250,000 multipolar electrogram snippets was selectively assembled to ensure representativity and quality before it was visually annotated by two operators, expert at recognizing dispersion and having reported AF termination rates ~ 90% in persistent AF population by ablating dispersed areas only (operators from the Substrate HD study). Operators analyzed 1.5 sec of multipolar electrograms and applied the definition of spatio-temporal dispersion as previously published: Dispersion areas were defined as clusters of electrograms, either fractionated or non-fractionated, that displayed interelectrode time and space dispersion at a minimum of 3 adjacent bipoles such that activation spread over all the AFCL. In the dispersion regions, a majority of electrograms were fractionated, bipoles exhibiting continuously fractionated signal were common and annotated as “dispersed”, a small proportion of non-fractionated electrograms were annotated as dispersed and fractionated electrograms without dispersion were annotated as “non dispersed”. VX1 underwent training and validation for the task of conducting real-time adjudication of multipolar electrograms for the presence or absence of dispersion. Then, the software was built to deliver adjudications in real time. Electrogram information is processed by a feature extraction module extracting features

related to local frequency and activation as well as EGM morphology, fractionation, and voltage, per single track. These features are analyzed by a trained Machine Learning algorithm to produce an array of dispersion likelihood A. In parallel, electrograms are processed by a trained deep learning algorithm producing an array of dispersion likelihood B. Both dispersion likelihood arrays are merged using a weighted average based on their agreement level to produce dispersion likelihood C. Array C is being color coded and displayed on the catheter schematic. To account for time-wise stability, several iterations in time are used to build a different color-coded list which is displayed on the upper frame of the software interface.

Devices and ablation protocol

The VX1 device is connected either to the LabSystem™ Pro EP Recording System (Boston Scientific) or the CardioLab™ EP Recording System (General Electric) for data acquisition.

A three-dimensional cardiac mapping system (Carto® 3, Biosense Webster or EnSite Precision™, Abbott or Rhythmia HDx™, Boston Scientific) was used to guide the procedures. Ablation was performed with the use of radiofrequency energy delivered by an irrigated-tip quadripolar ablation catheter (ThermoCool SmartTouch® SF, Biosense Webster or TactiCath™SE, Abbott or IntellaNav™, Boston Scientific).

These catheters were introduced through a long sheath (Fast-Cath Swartz SL0 Abbott, Inc.) and perfused with heparinized saline. Heparin was administered intravenously (goal: activated clotting time: 300-350 sec.). Esophageal temperature was monitored during the procedure (SensiTherm™ esophageal probe – Abbott). For patients in sinus rhythm (SR) at the outset of the procedure, AF was induced by rapid atrial pacing using the coronary sinus catheter (500-180ms). A reference AF cycle length (CL) value was determined as the average of two consecutive measurements of 10 CLs at the left and right atrial (LA and RA) appendages (LAA and RAA).

Baseline mapping in both atria was performed during AF with one of the following mapping multipolar catheter: the PentaRay® catheter spacing 2-6-2 (Biosense Webster), the Advisor™ HD Grid (Abbott), the Reflexion™ HD (Abbott), the Advisor™ FL (Lasso 10-pole, Abbott), the Lasso® Nav Eco catheter (Biosense Webster), the Intellamap Orion™ (Boston Scientific).

Study Endpoints and other sub-analysis

Ev-AIFib consisted in conducting both an acute and long-term evaluation of the feasibility and efficacy of VX1-enabled dispersion maps for the ablation of AF/AT:

(i) Feasibility and evaluation of the VX1 dispersion maps: Double blind comparison of VX1 and visual Dispersion maps (n=18 patients)

In a sub-set of 18 patients in AF (n=14) or AT (n=4), we compared Dispersion maps constructed simultaneously by two operators. The main operator tagged dispersion visually (blue tags)—without VX1, according to Seitz et al, (Seitz, Bars et al. 2017) while another operator was simultaneously tagging dispersed EGMS according to the indications provided by the VX1 software (white tags). Despite tagging simultaneously, each operator was blinded to the other operator's information. This was made possible by providing the VX1-tagging indications to the Carto/Precision engineer independently from the visual-tagging indications. Practically, the medical device screen was shut off for the main operator. Thus, VX1-guided tagging indications were provided without influencing the main operator's tagging and vice-versa. A combined VX1/operator map included information obtained simultaneously from VX1 and operator's visual analysis. The combined map was then reviewed by the main operator who analyzed both types of tagging (Visual and VX1-enabled). If white tags (VX1-enabled tagging) were not confirmed visually, their color was changed to yellow (considered as over detection by the software). Isolated blue tags were considered as under detection by the software. In this subgroup the regional discordance between the operator's visual interpretation and VX1 was more precisely evaluated than in reviewing all analyzed EGMs from the 3D shells. After the mapping was performed, the VX1-cued Dispersion maps (VX1-Maps) and visual maps were analyzed as follows:

- The concordance of VX1-Dispersion (white tags), and visual-Dispersion regions (blue tags), was characterized region per-region in 18 patients using the atrial segmentation presented in Supplementary Figure 1. Isolated blue tags and yellow tags are considered as discordant tags. Here, we only present data gathered after this post-mapping visual validation process.
- The total surface area in cm2 of the following regions were measured with the surface area estimation function in CARTO (n=9): the VX1 Dispersion regions (white tags), the visual Dispersion regions (blue tags), overlapping VX1-Dispersion/Visual-Dispersion regions, non-overlapping VX1-Dispersion/Visual-Dispersion regions.

(ii) Dispersion Regional Distribution Analysis

To evaluate the regional distribution of dispersion, we considered an analysis in each of the 22 regions presented in Supplementary Figure 1 in 58 patients. The analysis was conducted as follows:

1) We defined four levels (0 to 3) of dispersion density pertaining to a particular atrial sub-region:
   Level 0: no dispersion;
   Level 1: minimal dispersion;
   Level 2: moderate dispersion;
   Level 3: intense dispersion – at least half of the area under consideration was covered by dispersion tags.
2) For each sub-region, an average level was computed based on the entire population. This average level was transformed into a percentage (average level 3 corresponding to 100%).

(iii) A comparison of VX1-dispersion maps with CFAE maps was conducted (n = 27 patients).

We built CFAEs maps with the CARTO® V6. CFAE maps were constructed blindly to the main operator at the unadjusted, nominal out-of-the-box setting: 50-120 ms. This corresponded to a minimal and maximal thresholds set at ±0.05 millivolt (mV) and ±0.15 mV, respectively. The minimal and maximal intervals between two consecutive peaks were set at 50 msec and 120 msec, respectively. After the procedure, the VX1-enabled dispersion maps (VX1-Maps) and CFAE maps were compared. First, we measured the total surface area in cm^2 with the surface area estimation function in CARTO for the following regions: VX1 dispersion regions (white tags), CFAE regions (red/orange regions on the maps), overlapping dispersion/CFAE regions, non-overlapping dispersion/CFAE regions. Finally, each CFAE-map and VX1-map dispersion region was classified according to the atrial segmentation presented in Supplementary Figure 1. The concordance of dispersion and CFAE regions was then characterized region-per-region.

(iv) An evaluation of the effectiveness of VX1-based dispersion mapping and ablation, including acute AF termination rate and other procedural characteristics.

(v) The long-term effectiveness of VX1-based dispersion ablation in terms of freedom from arrhythmia recurrences.

(vi) Comparison of acute and log-term outcomes to the visual-dispersion guided control group of the Substrate-HD study.

Statistical Analysis

(i) Procedure Data comparison.

Continuous data were reported using mean ± standard deviation or median [interquartile range], and categorical data were reported using frequency counts and percentage. Crude comparisons of continuous data were performed using non-parametric Wilcoxon test or Welsh t-test; Chi-square test or Fisher exact tests were used for categorical data according to their distribution. All analyses were conducted using R version 4.0.0 (www.r-project.org). Differences with a two-tailed p value of less than 0.05 were considered statistically significant.

(ii) Comparison of VX1-enabled dispersion maps with CFAE maps.

CFAEs and dispersion VX1 surfaces were compared using the Wilcoxon Signed-Rank test for matched samples as previously described. Null hypothesis that the difference between medians of surface is 0 was tested against the alternative hypothesis that the difference is greater than 0 (i.e. H0: (median CFAEs surface – median dispersion VX1 surface) = 0, against H1: (median CFAEs surface – median dispersion VX1 surface) ≠ 0. The difference between CFAEs and dispersion VX1's joint surface and isolated surfaces was also compared using the same method (Wilcoxon signed-rank test). Regional concordance between CFAEs and dispersion VX1 was tested using Z-test for binomial dependent proportions as previously described. Null hypothesis that the two proportions are not different from 50% were tested against alternative hypothesis that proportions are different from 50% (i.e. H0: P=50% against H1:P≠50%).

(iii) Survival analyses

Kaplan–Meier curves were generated, and comparisons among groups were performed with the use of the log-rank test. A two-sided p value of less than 0.05 was considered for statistical significance.

(iv) Comparison of VX1 and visual Dispersion maps

Median surfaces were compared using the Wilcoxon Signed-Rank test for matched samples. Null hypothesis that the difference between medians is 0 was tested against the alternative hypothesis that the difference is greater than 0 (i.e., H0: (median DE VX1 surface – median DE visual surface) = 0, against H1: (median DE VX1 surface – median DE visual surface) ≠ 0.

Regional concordance between VX1 and operators' visual analysis was tested using Z-test for binomial dependent proportions. Null hypothesis that the two proportions are not different from 50% were tested against alternative hypothesis that proportions are different from 50%.

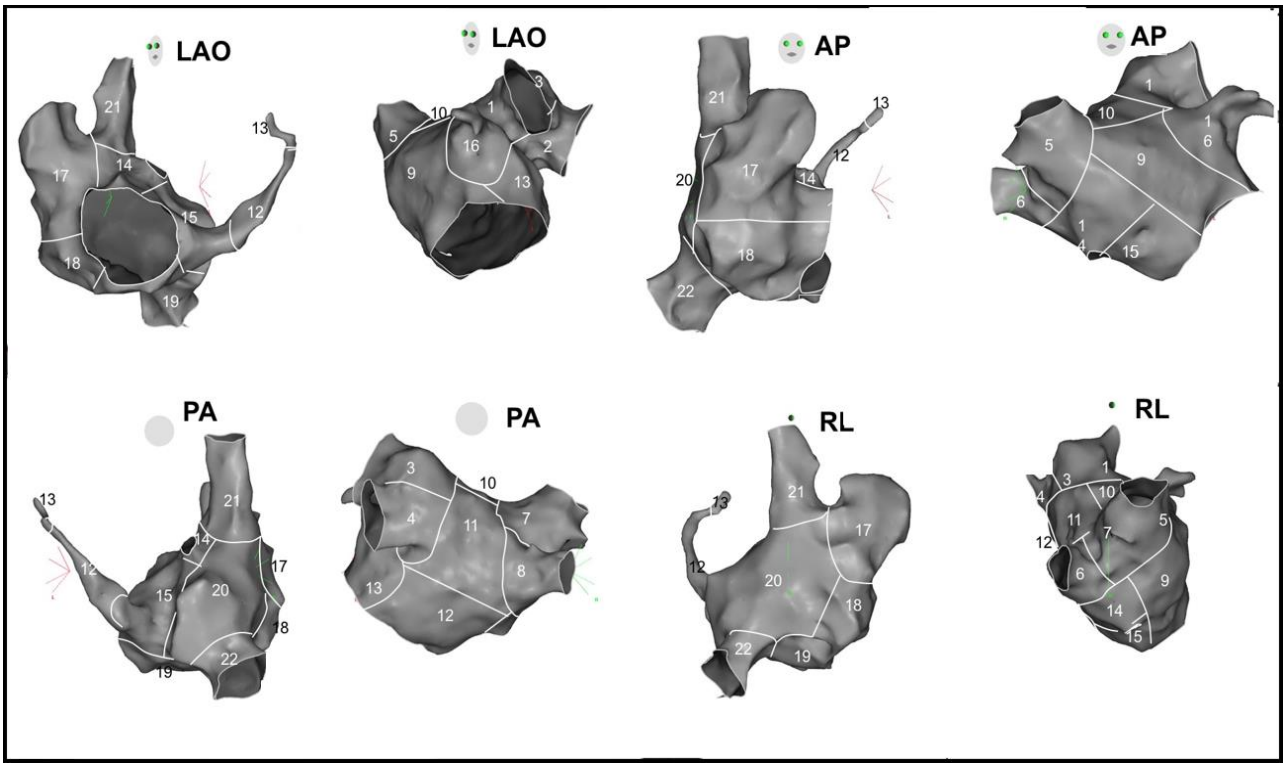

Supplementary Figure 1: Atrial segmentation used for characterization of dispersion tagged regions

Region 1: Left superior pulmonary vein anterior antrum – Ridge. Region 2: Left superior pulmonary vein inferior antrum-Ridge. Region 3: Left superior pulmonary vein posterior antrum. Region 4: Left inferior pulmonary vein posterior antrum. Region 5: Right superior pulmonary vein anterior antrum. Region 6: Right inferior pulmonary vein anterior antrum. Region 7: Right superior pulmonary vein posterior antrum. Region 8: Right inferior pulmonary vein posterior antrum. Region 9: Anterior wall from mitral annulus to roof. Region 10: Roof. Region 11: Posterior wall. Region 12: left atrial floor and mid-coronary sinus. Region 13: coronary sinus distal and mitral isthmus. Region 14: High septum. Region 15: Low septum. Region 16: Left atrial appendage. Region 17: Right atrial appendage. Region 18: Lateral right atrial appendage. Region 19: Cavo-tricuspid isthmus. Region 20: Posterior right atrium. Region 21: Superior vena cava. Region 22: Inferior vena cava

Supplementary Figures 2 and 3 (S2 and S3): Dispersion maps recapitulating the blue, red and orange colors presented in the interface.

S2: Representative examples: A: RA 3D shell; B: LA 3D shell C,D: Electrograms adjudicated as dispersed (C) or non-dispersed (D) and corresponding bipoles showing in red, orange (C) or in blue colors (D) in VX1 interface

S3: Cardiac electrophysiology lab configuration with 3D navigation (CARTO), intra-cardiac electrograms and VX1 interface: Left atrial shells and electrograms adjudicated as dispersed (A) or non-dispersed (B) and corresponding bipoles showing in red, orange (A) or in blue colors (B) in VX1.

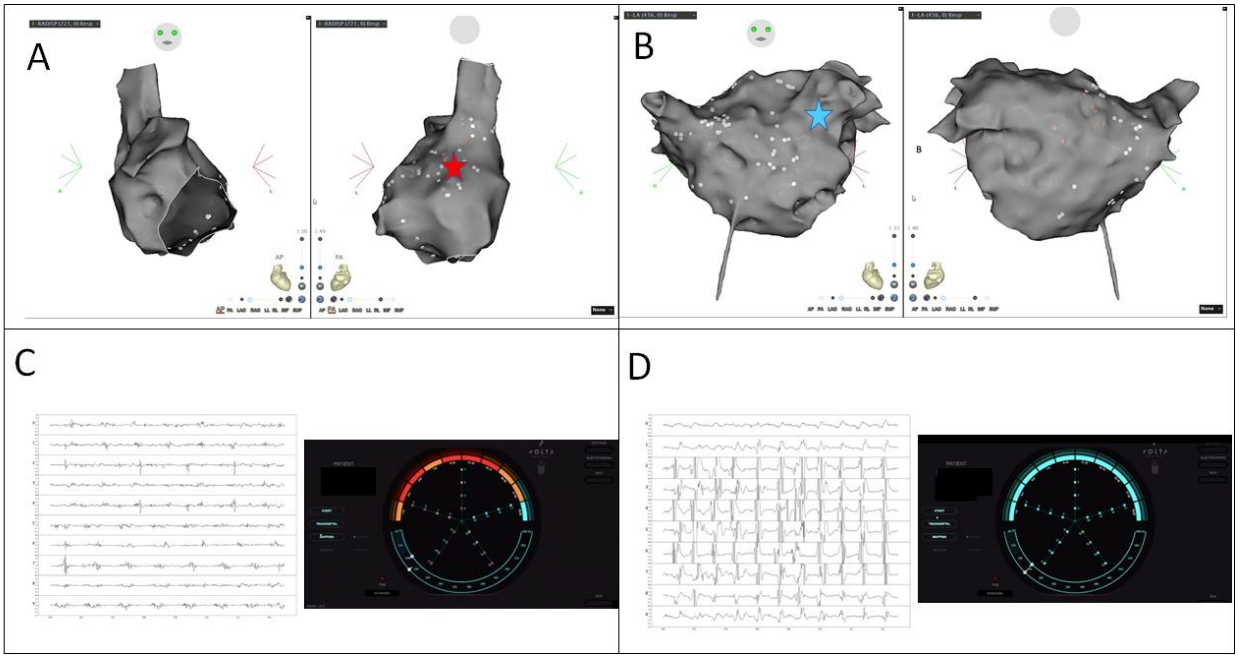

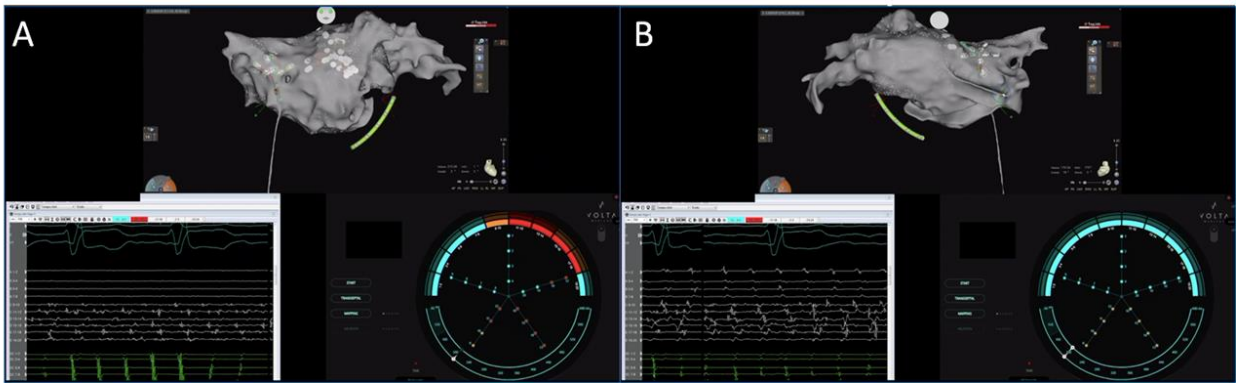

Results

(i) Evaluation of the VX1 software: comparison of VX1 and Visual Dispersion maps (n=18 patients)

Visual-maps/VX1 maps dispersion regional concordance/discordance (n=18 patients)

Here, each Visual-map and VX1-map dispersion region was classified according to the atrial segmentation presented in Supplementary Figure 1. Overall, 372 regions were analyzed (no right atrial mapping in 4 patients). 364 were concordant while 8 were discordant. The percentage of concordant regions is significantly superior to the one of discordant regions (test Z, H0: rate = 50%, p<.0001).

- Maps in two representative patients are presented in **Supplementary Figure 4** below.

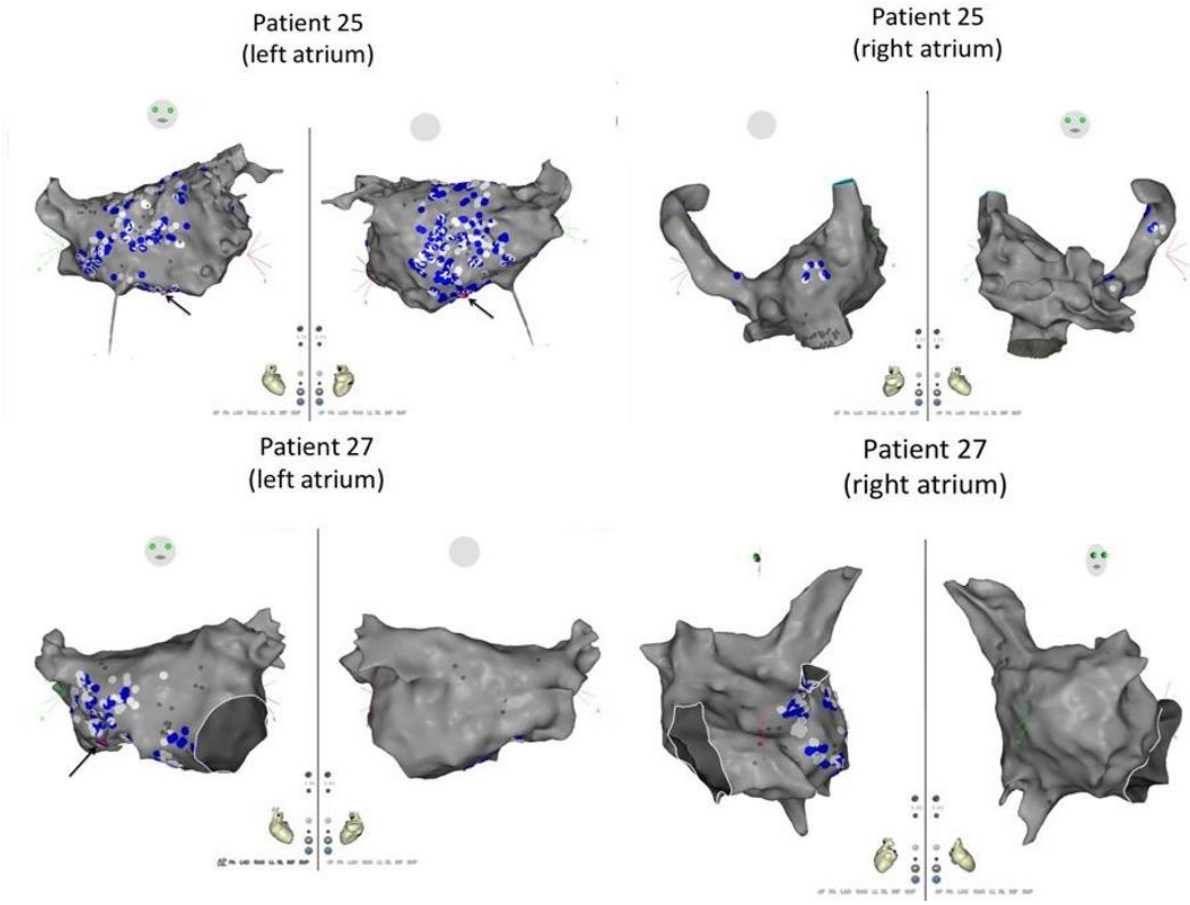

Supplementary Figure 4: *Visual-maps, VX1-maps presented in two representative patients.*

- Tag point size = size 2 (~2-mm radius)
- Blue tags : Visual-maps
- White tags : VX1-Maps
- Rose tags and black arrow: AF termination location

Comparison Visual-maps/VX1 maps dispersion region surface areas (n=9 patients)

We first measured the dispersion surface areas as determined in Visual-maps and in VX1 maps. Results are presented in **Supplementary Tables 1** and **2**. They indicate that Visual-maps and VX1-maps dispersion surface areas are quantitatively comparable with a non-significant tendency towards larger Visual-maps in the RA. Then, we quantified and compared the overlapping and non-overlapping Visual- and VX1 maps dispersion regions surface areas. Results presented below indicate that overlapping Visual-map and VX1 map surface areas are significantly larger than non-overlapping ones (p=0.0078, Wilcoxon test). Overall, this analysis indicates that Visual-map and VX1-map surface areas are closely related.

Supplementary Table 1: VX1- and Visual-maps dispersion regions surface areas (n=9 patients)

LA	**Surface area Visual-maps**	**Surface area VX1 maps**	**Differences**
Median [CI95]	3.65 [0.3-9.2]	3.65 [0-15]	1.05 [-0.3 – 5.8]
Wilcoxon Sign Rank Test for a paired dataset			0.0938 (Failure to reject Hypothesis H0)
RA	**Surface area Visual-maps**	**Surface area VX1 maps**	**Differences**
Median [CI95]	22.6 [10.2-54.8]	24.4 [12.4-56.3]	1.80 [-0.2 – 6.1]
Wilcoxon Sign Rank Test for a paired dataset			0.0547 (Failure to reject Hypothesis H0)

Supplementary Table 2: VX1- and Visual-maps dispersion regions overlapping surface areas (n=9 patients)

LA+RA	**Overlapping Visual- and VX1**	**Non-overlapping Visual-map**	**Non-overlapping VX1-map**	**Difference (Overlapping–Non-overlapping)**
Median [CI95]	24.4 [8.5-61.1]	2.3 [0-6.0]	5.6 [2.8-14.7]	16.6 [0.7-52.9]
Wilcoxon Sign Rank Test for paired and dependent data				0.0078 (Hypothesis H1 confirmed : Median≠0)
RA	**Overlapping Visual- and VX1**	**Non-overlapping Visual-map**	**Non-overlapping VX1-map**	**Difference (Overlapping–Non-overlapping)**
Median [CI95]	2.2 [0-8.2]	0.75 [0-1.6]	2.2 [0-6.8]	0.2 [-1.4 – 3.8]
Wilcoxon Sign Rank Test for paired and dependent data				0.8125 (Failure to reject Hypothesis H0)
LA	**Overlapping Visual- and VX1**	**Non-overlapping Visual-map**	**Non-overlapping VX1-map**	**Difference (Overlapping–Non-overlapping)**
Median [CI95]	20.2 [8.5-53.4]	1.4 [0-4.7]	4.6 [1.2-7.9]	14.5 [2.9-49.1]
Wilcoxon Sign Rank Test for paired and dependent data				0.0078 (Hypothesis H1 confirmed : Median≠0)

(ii) Dispersion Regional Distribution Analysis

To evaluate the regional distribution of dispersion, we considered an analysis in each of the 22 regions presented in **Supplementary Figure 1** in 58 patients. We analyzed the sub-regions 1-8 corresponding to the PV-antral regions as well as other non-PV regions (sub-regions 9-22). It was concluded that approximately 7% of the LA dispersion located in PV-antral sub-regions while the rest was distributed in other left atrial sub-regions. In **Supplementary Figures 5 and 6**, we present the percentage of patients with dispersion in each sub-region and the median level of dispersion in each atrial sub-region, respectively.

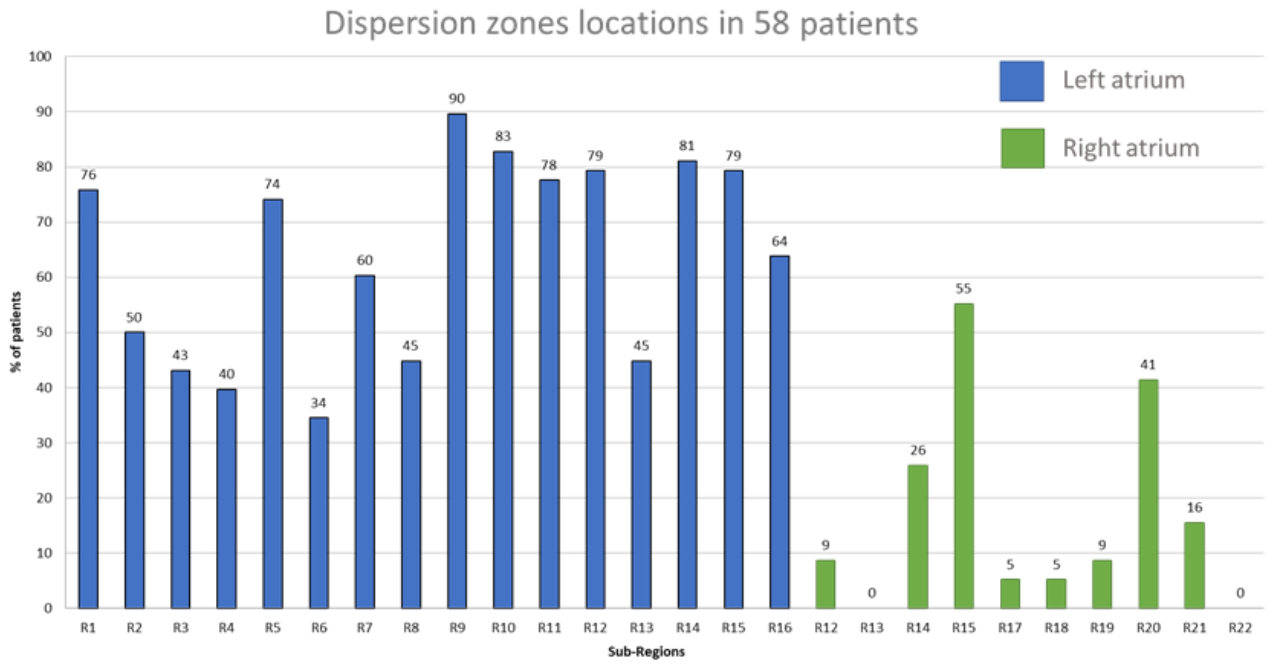

Supplementary Figure 5: *Percentage of patients with dispersion in each sub-region (according to Supplementary Figure 1)*

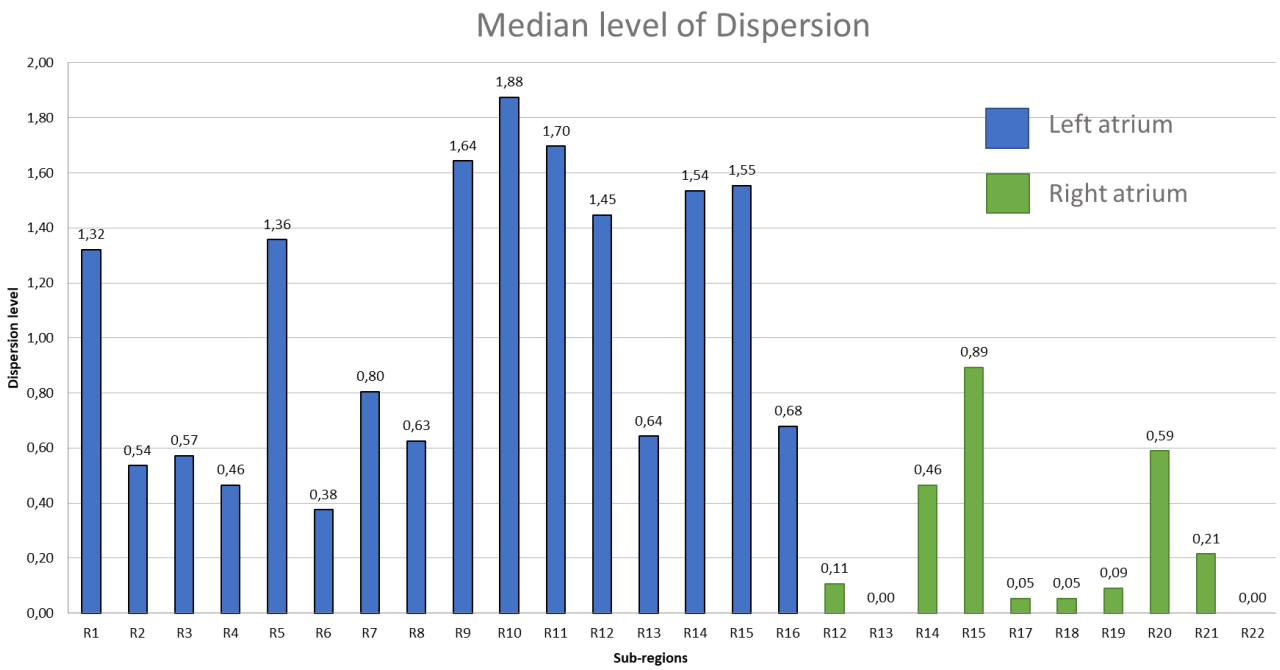

Supplementary Figure 6: *Median level of dispersion in each sub-region region (according to Supplementary Figure 1)*

(iii) VX1 and CFAE maps surface area analysis (n=27 patients)

As detailed in the Supplementary methods section, we constructed CFAEs maps using the CFAE module (Biosense Webster) and compared the surface area and the regional distribution of locations harboring the highest levels of CFAEs— orange/red regions on CFAEs maps— with the ones of VX1-tagged dispersion regions.

In two patients, representative examples of superimposed CFAEs-maps/VX1-maps are presented in **Supplementary Figure 7**.

We then conducted a comparison between the VX1 and CFAE maps surface areas and compared the VX1- and CFAEs-maps regions overlapping and non-overlapping surface areas (n=27 patients, respectively **Supplementary Tables 3 and 4**).

Supplementary Table 3 shows that VX1-maps surface areas are significantly smaller than CFAEs surface areas.

Supplementary Table 4 demonstrates that VX1- and CFAEs-maps regions overlapping surface areas (n=27 patients) are significantly smaller than non-overlapping surface areas.

Then, CFAEs-Maps/VX1 maps dispersion regional concordance/discordance was evaluated as described in the Supplementary methods section. Of 580 regions analyzed, 411 were concordant (70.9% [IC95 67.2-74.6%]) while 169 were discordant (29.1% [25.4-32.8%]. The concordance rate was significantly larger than the discordance (test Z, H0: proportion = 50%, <.0001). In summary, (i) VX1-map dispersion regions span a significantly smaller surface than CFAE regions. (ii) Albeit VX1-map dispersion regions and CFAE regions may be found in similar atrial sub-regions, non-overlapping CFAE/VX1 regions are significantly larger than overlapping ones.

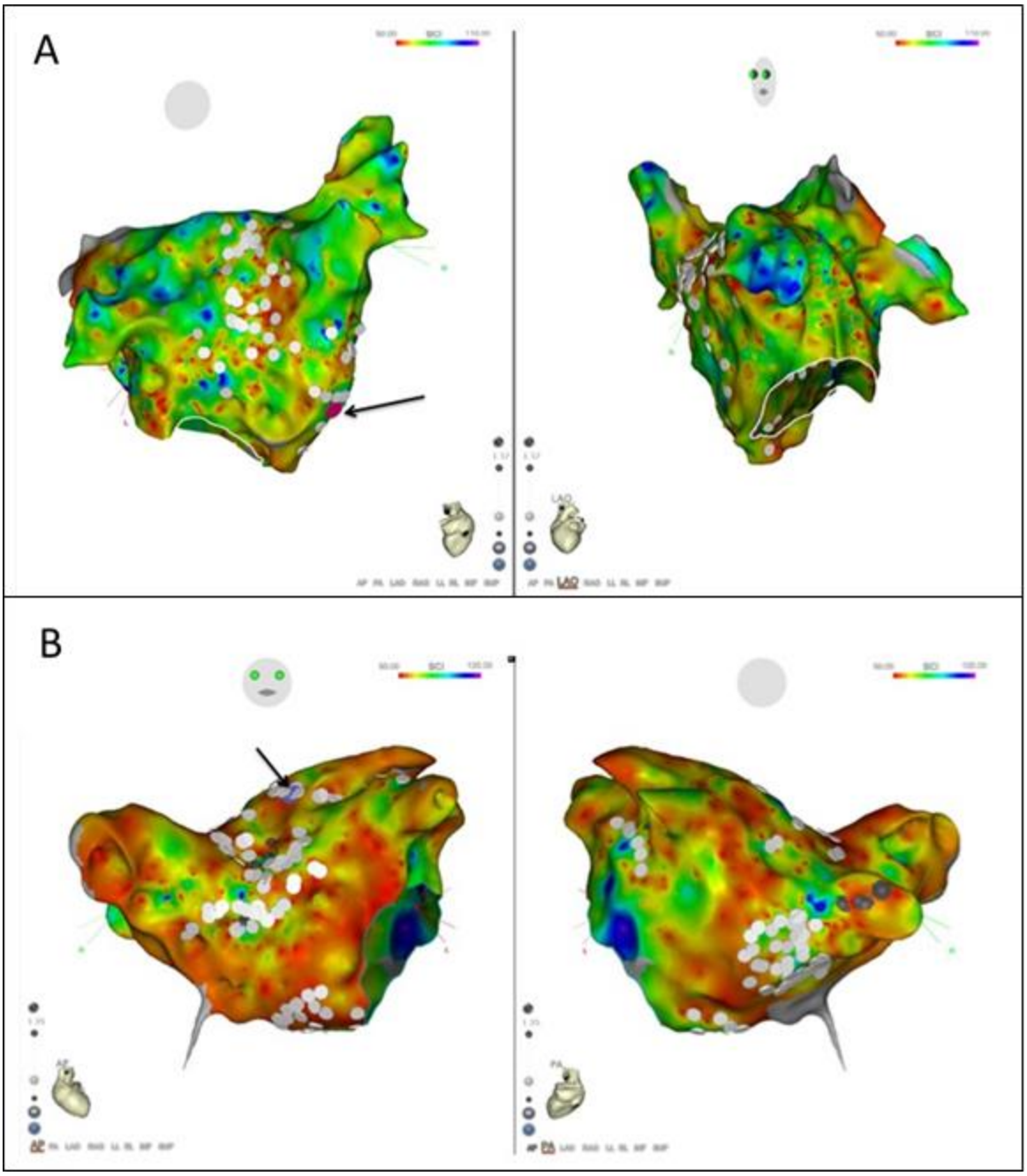

Supplementary Figure 7: Left atrial CFAE surface maps-VX1-maps representative examples from two patients (respectively upper and lower panels). White tags: VX1-maps. Red-orange color: highest level of CFAE EGMs. Pink tags and black arrow: AF termination location. Purple tags and black arrow: AT transition.

Supplementary Table 3: VX1- and CFAE maps surface area analysis (n=27 patients)

LA	**CFAE Surface area**	**VX1-map dispersion surface area**	**Difference**
Median [CI95]	45.4 [38.6-57.9]	26.4 [18.9-36.5]	19.2 [16.1-26.1]
Student Test for paired dependent variables			<.0001*
Wilcoxon Sign Rank Test for paired dependent variables			<.0001
RA	**CFAE Surface area**	**VX1-map dispersion surface area**	**Difference**
Median [CI95]	24.0 [18.6-32.0]	5.7 [3.3-8.4]	16.6 [13.5-21.5]
Wilcoxon Sign Rank Test for paired dependent variables			<.0001

*Differences follow a Gaussian distribution

Supplementary Table 4: VX1- and CFAEs-maps regions overlapping surface areas (n=27 patients)

LA+RA	**Overlapping CFAE- and VX1**	**Non-overlapping CFAE-map**	**Non-overlapping VX1-map**	**Difference (Overlapping–Non-overlapping)**
Median [CI95]	27.6 [18.1-34.3]	41.6 [31.2-55.4]	5.9 [4.5-6.8]	-23.4 [-30.0 ; -7.2]
Student Test for paired dependent variables				<.0001*
Wilcoxon Sign Rank Test for paired dependent variables				<.0001
RA	**Overlapping CFAE- and VX1**	**Non-overlapping CFAE-map**	**Non-overlapping VX1-map**	**Difference (Overlapping–Non-overlapping)**
Median [CI95]	4.1 [2.5-6.7]	18.9 [16.0-24.0]	1.7 [0.5-2.4]	-14.5 [-24.0 ; -10.3]
Wilcoxon Sign Rank Test for paired dependent variables				<.0001
LA	**Overlapping CFAE- and VX1**	**Non-overlapping CFAE-map**	**Non-overlapping VX1-map**	**Difference (Overlapping–Non-overlapping)**
Median [CI95]	21.0 [16.0-31.8]	24.0 [17.6-28.2]	3.6 [2.6-5.6]	-8.7 [-14.9 ; 3.3]
Wilcoxon Sign Rank Test for paired dependent variables				0.0527

*Differences follow a Gaussian distribution

(iv) Acute outcomes

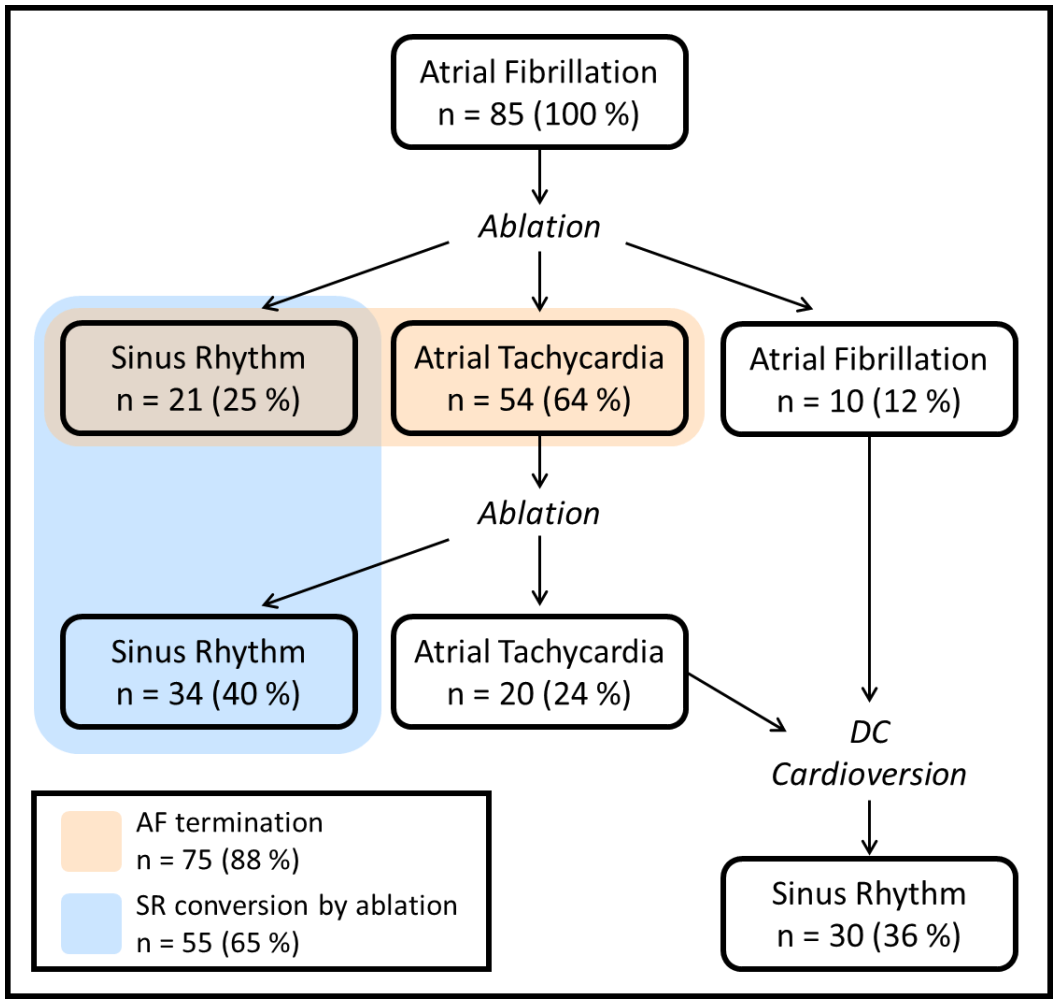

Supplementary Figure 8: Flow chart detailing acute outcomes in the Ev-AIFib trial. AF = Atrial Fibrillation; SR = Sinus Rhythm; DC = Direct Current.

(v) Freedom from Atrial Arrhythmias – Supplementary analysis

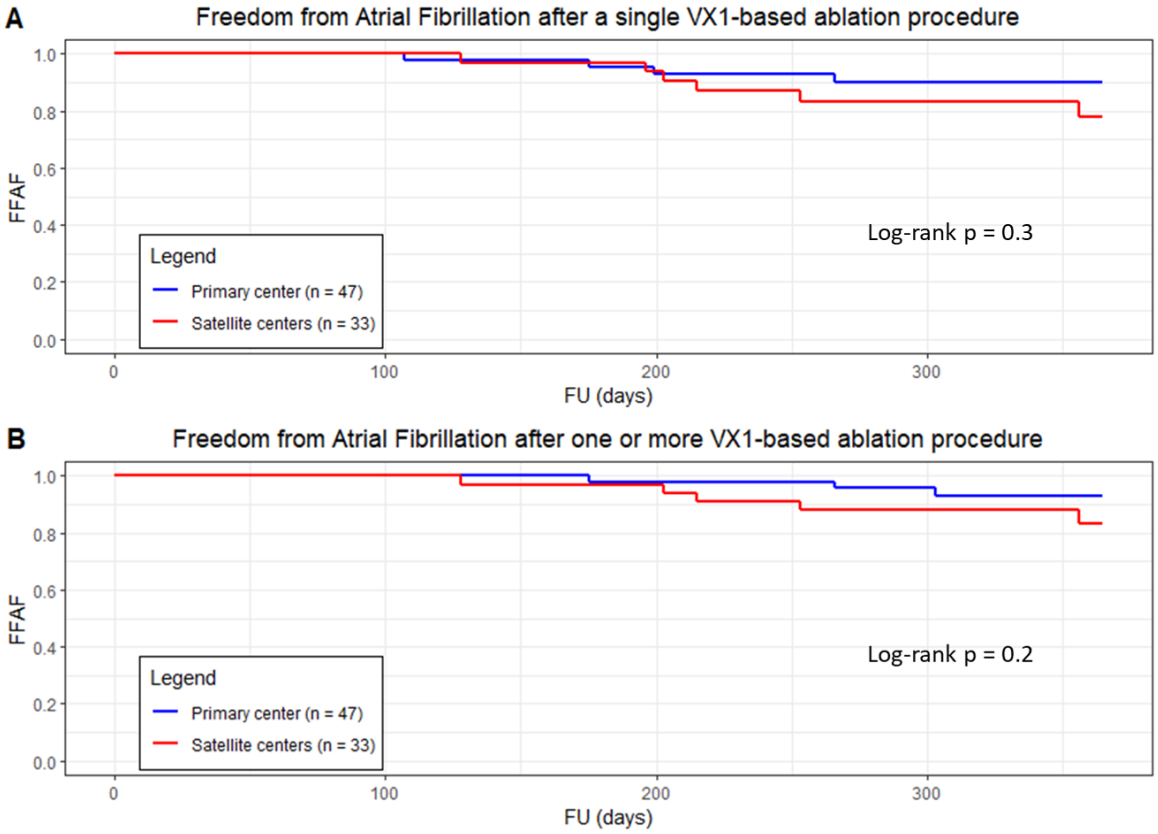

Supplementary Figure 9: *Kaplan–Meier estimates, for primary (blue) vs. satellite centers (red), of freedom from documented AF (A) after a single procedure (p = 0.3) and (B) after one or more procedures (p = 0.2), with or without the use of antiarrhythmic medications. A p-value < 0.05 was considered statistically significant.*

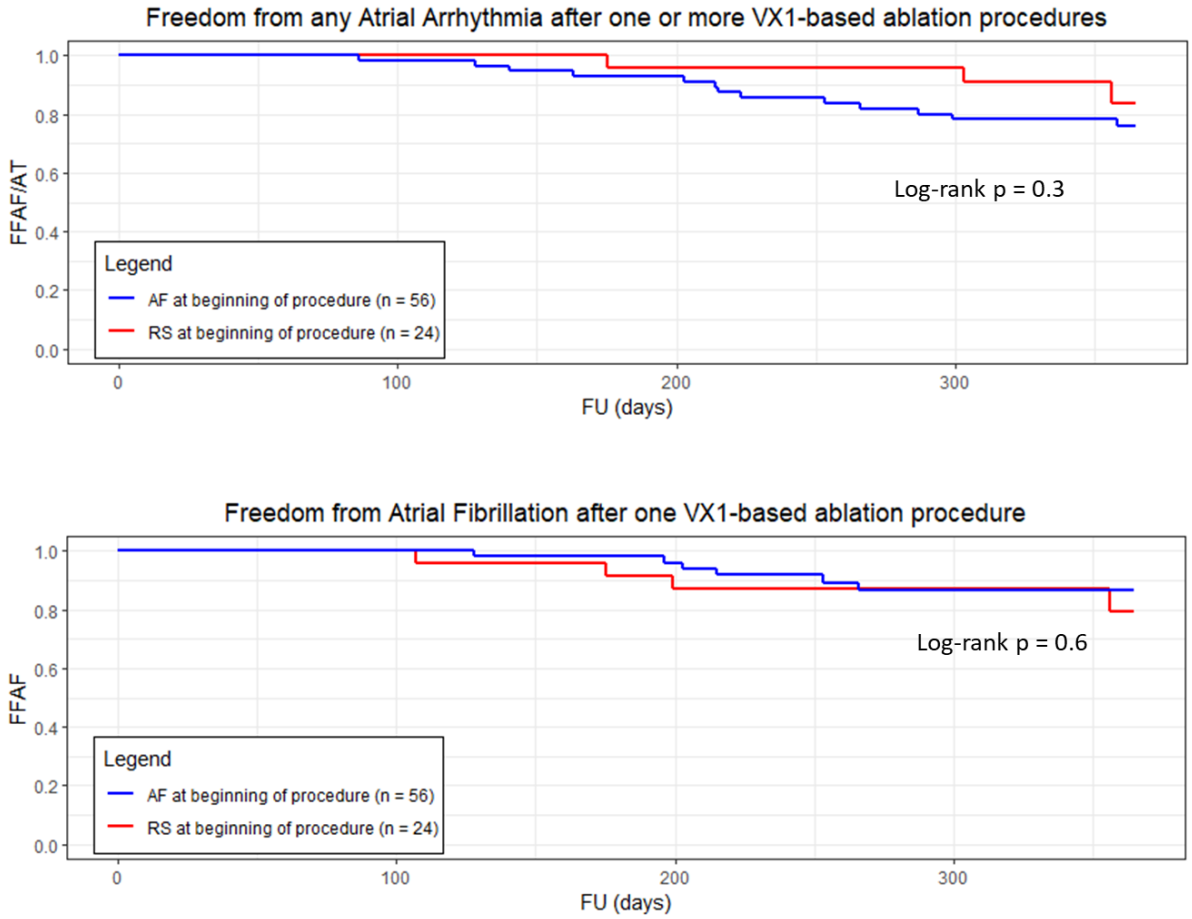

Supplementary Figure 10: *Kaplan–Meier estimates of (A) freedom from any documented atrial arrhythmia after one or more procedures or (B) freedom from AF after a single procedure, with or without the use of antiarrhythmic medications, for 2 groups of patients depending on the rhythm type (AF vs. RS) at beginning of the ablation procedure (In case of RS, the AF was induced) (p = 0.3 and p=0.6, respectively). A p-value < 0.05 was considered statistically significant.*

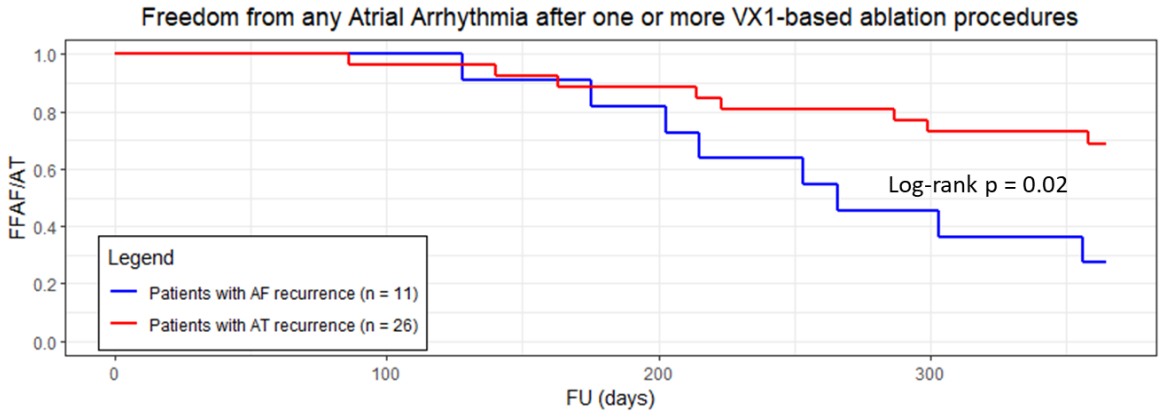

Supplementary Figure 11: *Kaplan–Meier estimates of freedom from any documented atrial arrhythmia after one or more procedures, with or without the use of antiarrhythmic medications, for 2 groups of patients depending on the type of recurrence after the index procedure: AF recurrence vs. AT recurrence (p = 0.02). A p-value < 0.05 was considered statistically significant.*

Catheters Configurations

For individual catheters the algorithm analysis is run on the following dipoles/spatial configuration.

Pentaray	K-2	K-1	**K**	K+1	K+2
1-2	17-18	19-20	**1-2**	3-4	5-6
3-4	19-20	1-2	**3-4**	5-6	7-8
5-6	1-2	3-4	**5-6**	7-8	9-10
7-8	3-4	5-6	**7-8**	9-10	11-12
9-10	5-6	7-8	**9-10**	11-12	13-14
11-12	7-8	9-10	**11-12**	13-14	15-16
13-14	9-10	11-12	**13-14**	15-16	17-18
15-16	11-12	13-14	**15-16**	17-18	19-20
17-18	13-14	15-16	**17-18**	19-20	1-2
19-20	15-16	17-18	**19-20**	1-2	3-4

Lasso 20	K-2	K-1	**K**	K+1	K+2
1-2	17-18	19-20	**1-2**	3-4	5-6
3-4	19-20	1-2	**3-4**	5-6	7-8
5-6	1-2	3-4	**5-6**	7-8	9-10
7-8	3-4	5-6	**7-8**	9-10	11-12
9-10	5-6	7-8	**9-10**	11-12	13-14
11-12	7-8	9-10	**11-12**	13-14	15-16
13-14	9-10	11-12	**13-14**	15-16	17-18
15-16	11-12	13-14	**15-16**	17-18	19-20
17-18	13-14	15-16	**17-18**	19-20	1-2
19-20	15-16	17-18	**19-20**	1-2	3-4

Lasso 10	K-2	K-1	**K**	K+1	K+2
1-2	9-10	10-1	**1-2**	2-3	3-4
2-3	10-1	1-2	**2-3**	3-4	4-5
3-4	1-2	2-3	**3-4**	4-5	5-6
4-5	2-3	3-4	**4-5**	5-6	6-7
5-6	3-4	4-5	**5-6**	6-7	7-8
6-7	4-5	5-6	**6-7**	7-8	8-9
7-8	5-6	6-7	**7-8**	8-9	9-10
8-9	6-7	7-8	**8-9**	9-10	10-1
9-10	7-8	8-9	**9-10**	10-1	1-2
10-1	8-9	9-10	**10-1**	1-2	2-3

HD Grid	K-2	K-1	**K**	K+1	K+2
B2-C2	A1-A2	B3-C3	**B2-C2**	A3-A4	B3-B4
A3-A4	B3-C3	B2-C2	**A3-A4**	B3-B4	C3-C4
B3-B4	B2-C2	A3-A4	**B3-B4**	C3-C4	D3-D4
C3-C4	A3-A4	B3-B4	**C3-C4**	D3-D4	D1-D2
D3-D4	B3-B4	C3-C4	**D3-D4**	D1-D2	C1-C2
D1-D2	C3-C4	D3-D4	**D1-D2**	C1-C2	B1-B2
C1-C2	D3-D4	D1-D2	**C1-C2**	B1-B2	A1-A2
B1-B2	D1-D2	C1-C2	**B1-B2**	A1-A2	B3-C3
A1-A2	C1-C2	B1-B2	**A1-A2**	B3-C3	B2-C2
B3-C3	B1-B2	A1-A2	**B3-C3**	B2-C2	A3-A4

Reflexion HD	K-2	K-1	**K**	K+1	K+2
1-2	17-18	19-20	**1-2**	3-4	5-6
3-4	19-20	1-2	**3-4**	5-6	7-8
5-6	1-2	3-4	**5-6**	7-8	9-10
7-8	3-4	5-6	**7-8**	9-10	11-12
9-10	5-6	7-8	**9-10**	11-12	13-14
11-12	7-8	9-10	**11-12**	13-14	15-16
13-14	9-10	11-12	**13-14**	15-16	17-18
15-16	11-12	13-14	**15-16**	17-18	19-20
17-18	13-14	15-16	**17-18**	19-20	1-2
19-20	15-16	17-18	**19-20**	1-2	3-4

Orion	K-2	K-1	**K**	K+1	K+2
B 4-5	D 5-6	C 5-6	**B 4-5**	C 3-4	D 3-4
C 3-4	C 5-6	B 4-5	**C 3-4**	D 3-4	E 3-4
D 3-4	B 4-5	C 3-4	**D 3-4**	E 3-4	F 3-4
E 3-4	C 3-4	D 3-4	**E 3-4**	F 3-4	G 4-5
F 3-4	D 3-4	E 3-4	**F 3-4**	G 4-5	F 5-6
G 4-5	E 3-4	F 3-4	**G 4-5**	F 5-6	E 5-6
F 5-6	F 3-4	G 4-5	**F 5-6**	E 5-6	D 5-6
E 5-6	G 4-5	F 5-6	**E 5-6**	D 5-6	C 5-6
D 5-6	F 5-6	E 5-6	**D 5-6**	C 5-6	B 4-5
C 5-6	E 5-6	D 5-6	**C 5-6**	B 4-5	C 3-4